

# Characterization of Alumina-Supported Pt-Ru Catalyst and Its Activities for Ethylene Hydrogenation and *n*-Butane Hydrogenolysis

On-line Number 1078

Saowapa Chotisuwan<sup>1</sup>, Jatuporn Wittayakun<sup>1</sup>, and Bruce C. Gates<sup>2</sup>

<sup>1</sup>School of Chemistry, Suranaree University of Technology, Nakhon Ratchasima, Thailand

<sup>2</sup>Department of Chemical Engineering and Materials Science, University of California, Davis, CA, USA

## ABSTRACT

Gamma-alumina supported bimetallic Pt-Ru catalyst (Pt-Ru/ $\gamma$ -Al<sub>2</sub>O<sub>3</sub>) was prepared by impregnation of Pt<sub>3</sub>Ru<sub>6</sub>(CO)<sub>21</sub>( $\mu_3$ -H)( $\mu$ -H)<sub>3</sub> cluster in CH<sub>2</sub>Cl<sub>2</sub> solution on  $\gamma$ -Al<sub>2</sub>O<sub>3</sub> and decarbonylated in helium at 300°C. Changes of the cluster before and after decarbonylation, monitored by infrared (IR) spectroscopy indicated that Pt<sub>3</sub>Ru<sub>6</sub>(CO)<sub>21</sub>( $\mu_3$ -H)( $\mu$ -H)<sub>3</sub> adsorbed strongly to surface of  $\gamma$ -Al<sub>2</sub>O<sub>3</sub> and could not be extracted from support by CH<sub>2</sub>Cl<sub>2</sub> solvent. In addition, Pt-Ru/ $\gamma$ -Al<sub>2</sub>O<sub>3</sub> was characterized by extended X-ray absorption fine structure (EXAFS) spectroscopy which confirmed that Pt and Ru were still intact after decarbonylation. Some changes in the cluster bonding were likely caused by cluster-support interaction. The catalyst was active for ethylene hydrogenation and *n*-butane hydrogenolysis. The temperature dependence of both reactions gave apparent activation energy of 8.4 ± 0.1 and 30.9 ± 0.1 kcal/mol, respectively.

## KEYWORDS

Bimetallic catalyst, Pt-Ru, alumina, ethylene hydrogenation, *n*-butane hydrogenolysis

## INTRODUCTION

Supported bimetallic catalysts have been reported in many applications, for instance, Pt-Re, Pt-Sn and Pt-Ir for naphtha reforming (Antos, et al., 1995), and Pt-Rh for auto exhaust conversion (Shelef and Graham, 1994). An incorporation of second metal to a supported platinum-group metal improves the catalyst performance and stability. In general, the simplest preparation method for bimetallic catalyst is by coimpregnation followed by high-temperature reduction. However, this conventional method gives nonuniform metal structure and usually with large particles on support. For better control of metal particles, bimetallic metal cluster with metal-metal bonds could be used as catalyst precursors to provide well-defined and/or highly dispersed bimetallic structure on support. In a bimetallic cluster consists of a noble metal and oxophillic metal combination, removal of ligands from adsorbed precursor gives the clusters of noble metals in clusters of oxides of the oxophillic metal which bonds strongly to oxide support and stabilized the dispersion of the metals (Alexeev, et al., 1996 and 2002).

The goal of this work was to prepare and characterize Pt-Ru/ $\gamma$ -Al<sub>2</sub>O<sub>3</sub> catalysts from a bimetallic cluster precursor, Pt<sub>3</sub>Ru<sub>6</sub>(CO)<sub>21</sub>( $\mu_3$ -H)( $\mu$ -H)<sub>3</sub> which contained Pt-Ru bond and its CO ligands could be easily removed by thermal treatment in an inert atmosphere. This precursor is in the same family as Pt<sub>2</sub>Ru<sub>4</sub>(CO)<sub>18</sub> which was successfully used as a catalyst precursor on  $\gamma$ -Al<sub>2</sub>O<sub>3</sub> by Alexeev and coworkers (2002).

The characterization methods for Pt-Ru/ $\gamma$ -Al<sub>2</sub>O<sub>3</sub> included infrared (IR), and extended X-ray absorption fine structure (EXAFS) spectroscopy. The Pt-Ru/ $\gamma$ -Al<sub>2</sub>O<sub>3</sub> was tested for ethylene hydrogenation

and *n*-butane hydrogenolysis. The first reaction is simple and widely used to test catalytic activity, while the latter reaction is sensitive to surface structure and can be used as a probe reaction.

## MATERIALS AND METHODS

The organometallic syntheses and supported catalyst preparations were performed in an argon drybox to prevent contact with moisture and air. The  $\gamma$ -Al<sub>2</sub>O<sub>3</sub> powder (Degussa, BET surface area 100 m<sup>2</sup>/g) was calcined in flowing O<sub>2</sub> at 400°C for 2 h and evacuated (pressure  $\approx 10^{-3}$  Torr) for 14 h before use. Hexane, and pentane (Fisher Scientific) were distilled over Na/benzophenone and purged with N<sub>2</sub> to eliminate oxygen. Gases (He and H<sub>2</sub>) were purified by passage through traps containing reduced Cu/Al<sub>2</sub>O<sub>3</sub> and zeolite particles to remove oxygen and water. Trace of water in dichloromethane was removed by molecular sieve 4Å. The Pt<sub>3</sub>Ru<sub>6</sub>(CO)<sub>21</sub>( $\mu_3$ -H)( $\mu$ -H)<sub>3</sub> was synthesized by a procedure described elsewhere (Adams, et al., 1994), and separated from other products by extraction with cold *n*-pentane. The cluster structure in CH<sub>2</sub>Cl<sub>2</sub> solution was confirmed by IR spectroscopy.

### Preparation of Pt-Ru/ $\gamma$ -Al<sub>2</sub>O<sub>3</sub> catalysts

The Pt-Ru/ $\gamma$ -Al<sub>2</sub>O<sub>3</sub> catalyst containing 1 wt% Pt and 1 wt% Ru was prepared by slurring of Pt<sub>3</sub>Ru<sub>6</sub>(CO)<sub>21</sub>( $\mu_3$ -H)( $\mu$ -H)<sub>3</sub> in CH<sub>2</sub>Cl<sub>2</sub> over  $\gamma$ -Al<sub>2</sub>O<sub>3</sub> powder for 1 day and evacuated for 1 day.

### Catalyst characterization

**Infrared Spectroscopy.** IR spectra of  $\gamma$ -Al<sub>2</sub>O<sub>3</sub> impregnated with Pt<sub>3</sub>Ru<sub>6</sub>(CO)<sub>21</sub>( $\mu_3$ -H)( $\mu$ -H)<sub>3</sub> were recorded before and after drying by a Bruker IFS-66v spectrometer with a resolution of 4 cm<sup>-1</sup>. Each sample was scanned 64 times and the signal averaged. For solid, small amount of powder samples were slightly pressed into semitransparent between KBr pellets placed in a cell in a glovebox.

**EXAFS Spectroscopy.** EXAFS experiments were performed at X-ray beamline X18B at the National Synchrotron Light Source, Brookhaven National Laboratory, New York, USA. The storage ring energy was 2.5 GeV and the ring current was in the range 80-220 mA. Sample wafers for transmission EXAFS spectroscopy in a special designed holder (Jentoft, et al., 1996) were cooled to nearly liquid nitrogen temperature before scanning at Pt L<sub>III</sub> edge (11564 eV) and Ru K edge (22117 eV) in transmission mode and integrating for 1 s at each energy in the range from 200 eV below the absorption edge to 975 eV beyond the edge. A double crystal monochromator Si(111) was used.

**EXAFS Data Analysis.** Because of the difference in energy between Pt L<sub>III</sub> edge (11564 eV) and Ru K edge (22117 eV), EXAFS data were collected at individual Pt L<sub>III</sub>, and Ru K absorption edge and analyzed with theoretical reference files. The interaction of Pt-Pt, Pt-Ru, Pt-O<sub>support</sub>, Ru-Ru, Ru-Pt, and Ru-O<sub>support</sub> bond were analyzed with phase shift and backscattering amplitudes calculated by FEFF software (Rehr, et al, 1991). The EXAFS data processing was carried out with Athena software (Raval, 2004). The final normalized EXAFS function from ATHENA software for each edge of each sample was obtained from the average of four scans. The EXAFS parameters were extracted from the raw data with the EXAFSPAK software (George, et al., 2000). The fitting were done in *R* space and *k* space with application of  $k^0$ ,  $k^1$ , and  $k^3$  weightings.

Raw EXAFS data obtained at Pt L<sub>III</sub> edge of Pt-Ru/ $\gamma$ -Al<sub>2</sub>O<sub>3</sub> prepared from Pt<sub>3</sub>Ru<sub>6</sub>(CO)<sub>21</sub>( $\mu_3$ -H)( $\mu$ -H)<sub>3</sub> after decarbonylation, were Fourier transformed over the ranges 3.25 <  $k$  < 14.25 with  $k^3$  weighting and no phase correction ( $k$  = the wave vector). The main contributions were isolated by backward Fourier transformation in the ranges 0.0 <  $R$  < 5.0 Å ( $R$  = interatomic distance from the absorber atom).

The raw data obtained at Ru K edge of  $\gamma$ -Al<sub>2</sub>O<sub>3</sub>-supported Pt<sub>3</sub>Ru<sub>6</sub>(CO)<sub>21</sub>( $\mu_3$ -H)( $\mu$ -H)<sub>3</sub> after decarbonylation, were analyzed over the ranges 3.40 <  $k$  < 14.45 and 0.0 <  $R$  < 4.0 Å.

The statistically justified number of free parameters estimated from Nyquist theorem for data obtained at Pt L<sub>III</sub> and Ru K edge of sample after decarbonylation were about 29 and 36, respectively.

## Catalyst Testing

**Ethylene Hydrogenation Reaction.** This study was carried out in a stainless steel U-tubed flow reactor at atmospheric pressure from -75 to -20°C. The sample was pretreated with He at 300°C for 2h prior to reaction testing. Typically, 10 to 20 mg of catalyst was diluted with 600 mg of inert  $\alpha$ -Al<sub>2</sub>O<sub>3</sub>, loaded into the reactor, and cooled to desired temperature before a gas mixture consisting of H<sub>2</sub>, ethylene, and balance He was flowed into reactor with 200 ml (NTP)/min flow rate. The effluent gas mixture was analyzed with an on-line gas chromatograph (Hewlett-Packard HP 6890) equipped with an Al<sub>2</sub>O<sub>3</sub> capillary column (50 m x 0.53 mm x 15.0 micron film thickness), and a flame ionization detector. Testing conditions included  $P_{\text{hydrogen}} = 80$  Torr,  $P_{\text{ethylene}} = 40$  Torr, and temperature varied from -75 to -20°C.

***n*-Butane Hydrogenolysis Reaction.** This test was performed in a quartz tube flow reactor at atmospheric pressure from 190 to 260°C. The sample was decarbonylated in the conditions as above. Typically, 25 - 30 mg of decarbonylated sample was diluted with inert  $\alpha$ -Al<sub>2</sub>O<sub>3</sub>, loaded into reactor, and heated to desired temperature before exposed to a flow of a gas mixture consisting of H<sub>2</sub>, *n*-butane, and balance He with 100 ml (NTP)/min flow rate. The effluent gas mixture was analyzed with the same on-line gas chromatograph. Testing conditions were:  $P_{\text{hydrogen}} = 540$  Torr,  $P_{\text{n-butane}} = 60$  Torr, and temperature varied from 190 to 260°C.

## RESULTS AND DISCUSSION

### Evidence of interaction of precursors with $\gamma$ -Al<sub>2</sub>O<sub>3</sub> from IR Spectroscopy

Figure 1 showed an IR spectrum in  $\nu_{\text{OH}}$  and  $\nu_{\text{CO}}$  regions of  $\gamma$ -Al<sub>2</sub>O<sub>3</sub> before and after interaction with Pt<sub>3</sub>Ru<sub>6</sub>(CO)<sub>21</sub>( $\mu_3$ -H)( $\mu$ -H)<sub>3</sub> cluster compared with that of the cluster dissolved in CH<sub>2</sub>Cl<sub>2</sub>. The bands at 3786, 3728 and 3672 cm<sup>-1</sup> of bared  $\gamma$ -Al<sub>2</sub>O<sub>3</sub> (spectrum 1 in Figure 1A) were assigned to different types of isolated hydroxyl groups (Alexeev, et al., 2002). The peak at 3786 cm<sup>-1</sup> was assigned to type Ib, (Al<sup>3+</sup><sub>oct</sub>)OH while the peak at 3728 cm<sup>-1</sup> was assigned to type IIa, (Al<sup>3+</sup><sub>tet</sub>)(OH)(Al<sup>3+</sup><sub>oct</sub>). (Mestl and Knözinger, 1997). The broad at 3579 cm<sup>-1</sup> represents hydrogen-bonded OH groups (Alexeev, et al., 2002 and references therein). The spectrum of vacuum-dried mixture of Pt<sub>3</sub>Ru<sub>6</sub>(CO)<sub>21</sub>( $\mu_3$ -H)( $\mu$ -H)<sub>3</sub> and  $\gamma$ -Al<sub>2</sub>O<sub>3</sub> at 25°C showed only two broad peaks at 3679 and 3587 cm<sup>-1</sup> in the hydroxyl region ((spectrum 2 in Figure 1A)). The change in hydroxyl peaks indicated that they involved in the interaction with the cluster.

Four peaks in carbonyl range were observed at 2081, 2065, 2048 and 2023 cm<sup>-1</sup> for Pt<sub>3</sub>Ru<sub>6</sub>(CO)<sub>21</sub>( $\mu_3$ -H)( $\mu$ -H)<sub>3</sub> in CH<sub>2</sub>Cl<sub>2</sub> solution (spectrum 2 in Figure 1B). After it was impregnated on  $\gamma$ -Al<sub>2</sub>O<sub>3</sub> and dried in

vacuum, carbonyl peaks were still present at 2137, 2073, 2038 and 2011  $\text{cm}^{-1}$  (spectrum 2 in Figure 1B). The small peak at 2137  $\text{cm}^{-1}$  was likely due to monometallic complex containing terminal carbonyl from cluster decomposition, such as  $\text{Pt}^{\text{II}}\text{-CO}$  and/or  $\text{Ru-CO}$  adsorbed on  $\gamma\text{-Al}_2\text{O}_3$  (Hadjiivanov and Vayssilov, 2002). Whereas the other three peaks corresponded to carbonyl peaks in the cluster interacting with alumina support. The frequency was shifted to lower value due to weakening of C-O bond after interacting with hydroxyl group of alumina. This interaction was suspected because the change of hydroxyl bands was coincident with the shift of carbonyl bands in the cluster.

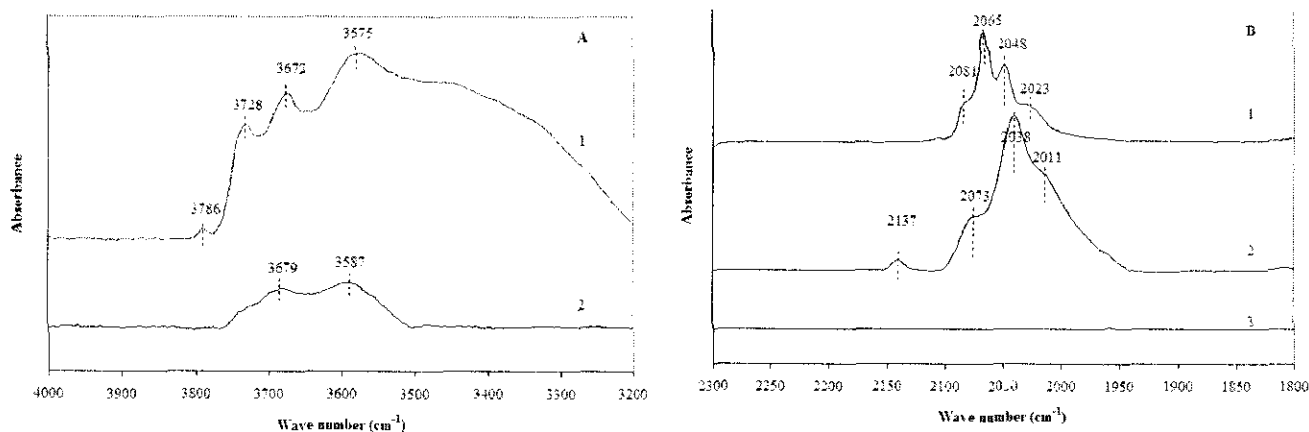


**Figure 1. (A) IR spectrum in  $\nu_{\text{OH}}$  region: (1) Bared  $\gamma\text{-Al}_2\text{O}_3$  calcined at  $400^\circ\text{C}$  for 14 h; (2) dried  $\text{Pt}_3\text{Ru}_6(\text{CO})_{21}(\mu_3\text{-H})(\mu\text{-H})_3$  on  $\gamma\text{-Al}_2\text{O}_3$ . (B) Infrared in  $\nu_{\text{CO}}$  regions: (1)  $\text{Pt}_3\text{Ru}_6(\text{CO})_{21}(\mu_3\text{-H})(\mu\text{-H})_3$  dissolved in dichloromethane; (2)  $\text{Pt}_3\text{Ru}_6(\text{CO})_{21}(\mu_3\text{-H})(\mu\text{-H})_3$  adsorbed on  $\gamma\text{-Al}_2\text{O}_3$  after removal of solvent; (3) sample after decarbonylation with He at  $300^\circ\text{C}$  for 2 h.**

An attempt to extract the cluster  $\text{Pt}_3\text{Ru}_6(\text{CO})_{21}(\mu_3\text{-H})(\mu\text{-H})_3$  from  $\gamma\text{-Al}_2\text{O}_3$  with  $\text{CH}_2\text{Cl}_2$  was not successful because the cluster adsorbed strongly on alumina surface. There were two possible interactions between carbonyl ligands and  $\gamma\text{-Al}_2\text{O}_3$  support: (1) between carbonyl oxygen and surface hydroxyl proton to form hydrogen-bonding; (2) between carbonyl oxygen and Lewis acid sites ( $\text{Al}^{3+}$  ions). After treating the dried mixture with He at  $300^\circ\text{C}$  for 2 h, all  $\nu_{\text{CO}}$  bands disappeared, indicating complete decarbonylation. Carbonylation was a conversion of coordinated CO ligands with basic surface sites ( $\text{O}^{2-}$  or  $\text{OH}$ ) to carbon dioxide (Alexeev, et al., 2002).

The interaction between carbonyl ligands and surface hydroxyl groups may be formed by nucleophilic displacement of carbonyl which is energetically favored for  $\gamma\text{-Al}_2\text{O}_3$ -supported metal carbonyls. This decarbonylation was resulted from cleavage of CO ligands of metal carbonyl and formed metal- $\text{O}_{\text{support}}$  bonds (Myllyoja, et al., 1999) and caused a formation of anionic metal carbonyl clusters (Alexeev, et al., 2002). Typically, the formation of anionic metal carbonyl clusters shows the shifting of terminal  $\nu_{\text{CO}}$  bands to lower frequencies (Gates, 1998). However, IR data does not show any anionic species of metal carbonyl cluster on support. However, it was possible that some of surface species after contact  $\gamma\text{-Al}_2\text{O}_3$  with  $\text{Pt}_3\text{Ru}_6(\text{CO})_{21}(\mu_3\text{-H})(\mu\text{-H})_3$  were the fragments of  $\text{Pt}_3\text{Ru}_6(\text{CO})_{21}(\mu_3\text{-H})(\mu\text{-H})_3$  that had been decarbonylated and coordinated to oxygen atoms on  $\gamma\text{-Al}_2\text{O}_3$  surface.

## Characterization of alumina Pt-Ru catalysts by EXAFS Spectroscopy

EXAFS data of Pt-Ru/ $\gamma$ -Al<sub>2</sub>O<sub>3</sub> give information of local structure such as coordination number of absorbing atom and interatomic distances between absorbing atom and scattering atoms. The EXAFS data analysis of these samples at Pt L<sub>III</sub> edge and Ru K edge were summarized in Table 1. The estimated accuracies of coordination number (*N*), distance (*R*), Debye-Waller factor ( $\Delta\sigma^2$ ), and inner potential ( $\Delta E_0$ ) are as follows:  $\pm 20\%$ ,  $\pm 1\%$ ,  $\pm 30\%$ ,  $\pm 10\%$ , respectively. After decarbonylation in He at 300°C for 2 h, the EXAFS results of Pt-Ru prepared from cluster precursor gave a Pt-Pt interatomic distance of 2.64 Å which was nearly similar to that of Pt<sub>3</sub>Ru<sub>6</sub>(CO)<sub>21</sub>( $\mu_3$ -H)( $\mu$ -H)<sub>3</sub>, average 2.63 Å. (Adams, et al, 1994). The Pt-Pt had coordination number of 1.7, lower than 2.0 in the precursor. The Pt-Ru contribution in Pt-Ru/ $\gamma$ -Al<sub>2</sub>O<sub>3</sub> had interatomic distance of 2.68 Å, slightly shorter than the average 2.80 Å in the precursor in crystalline form. The coordination number of the first shell of Pt-Ru contribution compared with that of precursor decreased from 4.0 to 2.2. The Pt-O<sub>s</sub> contribution was found at 2.07 Å for interatomic distance and coordination number of 2.3.

The EXAFS results at Ru K edge showed Ru-Ru distance of 2.62 Å, decreased from 3.04 Å of Ru-Ru distance in the precursor. The shorter distance could be resulted from the loss of bridging hydride ligands bonded to Ru<sub>3</sub> faces after decarbonylation. The EXAFS results showed nearly the same of Ru-Ru coordination number for cluster adsorbed on support after decarbonylation and that for precursor in crystalline form, 2.4 and 2.1, respectively. The average coordination numbers of Ru-Pt contribution of cluster after decarbonylation decreased from 2.0 to 1.0. EXAFS results confirmed metal-metal framework remained intact on alumina support after decarbonylation, the cluster-support interaction was not strong enough to break cluster framework.

**Table 1. Summary of EXAFS data of  $\gamma$ -Al<sub>2</sub>O<sub>3</sub>-supported Pt<sub>3</sub>Ru<sub>6</sub>(CO)<sub>21</sub>( $\mu_3$ -H)( $\mu$ -H)<sub>3</sub> after decarbonylation with He at 300°C for 2 h.**

Edge	Shell	<i>N</i>	<i>R</i> (Å)	10 <sup>3</sup> × $\Delta\sigma^2$ (Å <sup>2</sup> )	$\Delta E_0$ (eV)
Pt L <sub>III</sub>	Pt-Pt	1.7	2.64	3.0	-4.6
	Pt-Ru	2.2	2.68	4.2	6.4
	Pt-O <sub>s</sub>	2.3	2.07	12.0	8.1
	Pt-O <sub>l</sub>	0.8	2.99	-2.4	-7.6
Ru K	Ru-Ru	2.1	2.62	4.1	-13.3
	Ru-Pt	1.0	2.68	4.5	-12.3
	Ru-O <sub>s</sub>	1.2	2.06	10.9	4.9
	Ru-O <sub>l</sub>	2.1	2.89	0.1	11.8

Notation: the subscript s and l refer to short and long, respectively

## Catalyst Testing for Ethylene Hydrogenation and *n*-Butane Hydrogenolysis

The Pt-Ru/ $\gamma$ -Al<sub>2</sub>O<sub>3</sub> prepared from the cluster precursor was treated by decarbonylation in He at 300°C for 2h prior to test catalytic reactions. The raw data were collected at steady-state operation and represented in units of mol of ethylene converted (g catalyst·s)<sup>-1</sup> (Figure 2A and 2B). Figure 2A shows Arrhenius plot of ethylene hydrogenation over  $\gamma$ -Al<sub>2</sub>O<sub>3</sub>-supported Pt<sub>3</sub>Ru<sub>6</sub>(CO)<sub>21</sub>( $\mu_3$ -H)( $\mu$ -H)<sub>3</sub> under catalysis condition of  $P_{\text{ethylene}} = 40$  Torr,  $P_{\text{hydrogen}} = 80$  Torr; total feed flow rate: 200 ml (NTP)/min; catalyst mass: 10 mg, 1 wt% Pt and 1 wt% Ru, and temperature = -75 to -20°C.

The result for these reactions was summarized in Table 2. The catalytic activity of ethylene hydrogenation in terms of turn over frequency (TOF) at  $-40^{\circ}\text{C}$  of Pt-Ru/ $\gamma\text{-Al}_2\text{O}_3$  catalysts prepared from  $\text{Pt}_3\text{Ru}_6(\text{CO})_{21}(\mu_3\text{-H})(\mu\text{-H})_3$  was  $6.5 \times 10^{-4} \pm 0.1$ . The apparent activation energy obtained from temperature dependence of ethylene hydrogenation reaction for this catalyst was  $8.4 \pm 0.1$  kcal/mol. This value is comparable to that reported for ethylene hydrogenation catalyzed by Pt catalysts, and Ru catalysts consisting of metallic particles on metal oxide supports (Dorling, et al., 1969; Hwang, et al., 2003).

From this catalytic data, it can be concluded that this catalyst prepared from the molecular precursor is very active for ethylene hydrogenation, which is structural insensitive. In addition, there was no sign of catalyst deactivation during the test period.

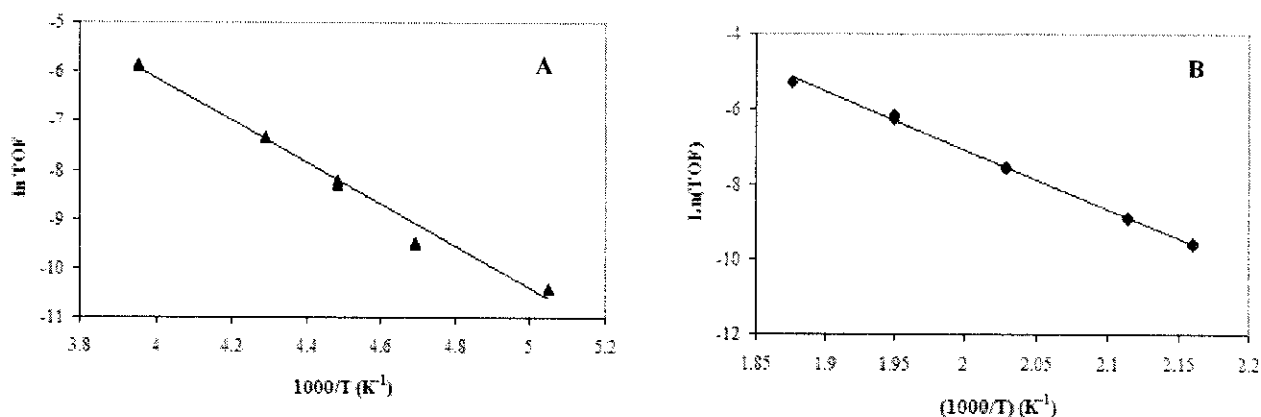


**Figure 2.** Arrhenius plot for (A) ethylene hydrogenation catalyzed by PtRu/ $\gamma\text{-Al}_2\text{O}_3$  prepared from  $\text{Pt}_3\text{Ru}_6(\text{CO})_{21}(\mu_3\text{-H})(\mu\text{-H})_3$ ; reaction condition:  $P_{\text{ethylene}} = 40$  Torr,  $P_{\text{hydrogen}} = 80$  Torr; total feed flow rate: 200 ml (NTP)/min; catalyst mass: 10 mg, 1 wt% Pt and 1 wt% Ru. (B) *n*-Butane hydrogenolysis; reaction condition:  $P_{n\text{-butane}} = 60$  Torr,  $P_{\text{hydrogen}} = 540$  Torr; total feed flow rate: 100 ml (NTP)/min; catalyst mass: 26 mg, 1 wt% Pt and 1 wt% Ru.

**Table 2.** Ethylene hydrogenation and *n*-butane hydrogenolysis catalyzed by  $\gamma\text{-Al}_2\text{O}_3$ -supported PtRu catalysts treated in He at  $300^{\circ}\text{C}$  for 2 h

Ethylene hydrogenation		<i>n</i> -Butane hydrogenolysis				
Activity	Apparent activation	Activity	Apparent activation	Product distribution (%) <sup>d</sup>		
TOF $\times 10^4$ (s <sup>-1</sup> ) <sup>c</sup>	Energy (kcal/mol)	TOF $\times 10^4$ (s <sup>-1</sup> ) <sup>d</sup>	Energy (kcal/mol)	CH <sub>4</sub>	C <sub>2</sub> H <sub>6</sub>	C <sub>3</sub> H <sub>6</sub>
$6.5 \pm 0.1$	$8.4 \pm 0.1$	$5.2 \pm 0.2$	$30.9 \pm 0.1$	33	63	4

<sup>c</sup> Reaction at  $-40^{\circ}\text{C}$ ,  $P_{\text{ethylene}} = 40$  Torr and  $P_{\text{hydrogen}} = 200$  Torr.

<sup>d</sup> Reaction at  $220^{\circ}\text{C}$ ,  $P_{n\text{-butane}} = 60$  Torr and  $P_{\text{hydrogen}} = 540$  Torr

For *n*-butane hydrogenolysis reaction, the catalytic activity in terms of turn over frequency (TOF) at  $220^{\circ}\text{C}$  of this Pt-Ru/ $\gamma\text{-Al}_2\text{O}_3$  catalyst was found to be  $5.2 \times 10^{-4} \pm 0.2$ . The apparent activation energy obtained from temperature dependence was  $30.9 \pm 0.1$  kcal/mol. This value is approximately the same as the value reported for *n*-butane hydrogenolysis catalyzed by Pt and Ru catalysts consisting of metallic particles on metal oxide supports (Bond and Slaa, 1995; Bond and Cunningham 1996). Product distribution percentages or selectivity in table 2 at  $220^{\circ}\text{C}$ , indicate high selectivity for ethane. However, selectivity for

CH<sub>4</sub> is much higher than that for C<sub>3</sub>H<sub>8</sub>, this can be suggested that multiple hydrogenolysis occurred over this bimetallic catalyst in *n*-butane hydrogenolysis.

From catalytic testing of Pt-Ru/ $\gamma$ -Al<sub>2</sub>O<sub>3</sub>, the catalyst which was prepared from the molecular precursor was active for *n*-butane hydrogenolysis, which is structural sensitive. Again, there was no sign of catalyst deactivation during the test period.

## CONCLUSIONS

The characterization of  $\gamma$ -Al<sub>2</sub>O<sub>3</sub>-supported Pt<sub>3</sub>Ru<sub>6</sub>(CO)<sub>21</sub>( $\mu_3$ -H)( $\mu$ -H)<sub>3</sub> were carried out by IR and EXAFS spectroscopy. The data suggested that Pt<sub>3</sub>Ru<sub>6</sub>(CO)<sub>21</sub>( $\mu_3$ -H)( $\mu$ -H)<sub>3</sub> adsorbed strongly on surface of  $\gamma$ -Al<sub>2</sub>O<sub>3</sub> by nucleophilic displacement between coordinated CO ligands of precursor and surface hydroxyl group on support. Decarbonylation occurred by the cleavage of CO ligands of metal carbonyl upon heating and resulted metal-O<sub>support</sub> bonds forming partially decarbonylated surface species on  $\gamma$ -Al<sub>2</sub>O<sub>3</sub> surface. The carbonyl ligands can be removed completely in flowing He at 300°C for 2h to give bimetallic Pt-Ru/ $\gamma$ -Al<sub>2</sub>O<sub>3</sub>. Results from EXAFS spectroscopy confirmed that Pt and Ru were still intact after decarbonylation.

Pt-Ru/ $\gamma$ -Al<sub>2</sub>O<sub>3</sub> from a molecular precursor was active for both ethylene hydrogenation and *n*-butane hydrogenolysis.

## ACKNOWLEDGMENTS

We thank Prof. Neil E. Schore at Department of Chemistry, University of California, Davis, CA, USA, for UV lamp used to synthesize the molecular precursor. The EXAFS experiments were performed at the National Synchrotron Light Source at Brookhaven National Laboratory, Upton, New York. The EXAFS data were processed with ATHENA software developed by Bruce Ravel, and analyzed with EXAFSPAK software developed by George, G. N., et al.

## REFERENCES

- Adams, R. D., Barnard, T. S., Li, Z., Wu, W., Yamamoto, J.; "Cluster Synthesis. 43. New Layer-Segregated Platinum-Ruthenium Cluster Complexes and Their Reactions with Diphenylacetylene," *Organometallics*, 13, 2357-2364 (1994)
- Alexeev, O., Graham, G. W., Shelef, M., Adams, R. D., Gates, B. C.; " $\gamma$ -Al<sub>2</sub>O<sub>3</sub>-Supported PtRu Clusters Prepared from [Pt<sub>2</sub>Ru<sub>4</sub>(CO)<sub>18</sub>]: Characterization by Infrared and Extended X-ray Absorption Fine Structure Spectroscopies," *J. Phys. Chem. B*, 106, 4697-4704 (2002)
- Alexeev, O., Shelef, M., Gates, B. C.; "MgO-Supported Platinum-Tungsten Catalysts Prepared from Organometallic Precursors: Platinum Clusters Isolated on Dispersed Tungsten," *J. Catal.*, 164, 1-15 (1996)
- Antos, G. A., Aitani, A. M., Parera, J. M., Eds, "Catalytic naphtha Reforming," Marcel Dekker, New York (1995)
- Bond, G. B., Cunningham, R. H., "Alkane Transformations on Supported Platinum Catalysts, Part 3: the Stability of Pt/Al<sub>2</sub>O<sub>3</sub> (EUROPT-3) and of Pt/Al<sub>2</sub>O<sub>3</sub> (EUROPT-3) during the hydrogenolysis of Alkanes," *J. Catal.* 163, 328-337 (1996)

- Bond, G. B., Slaat, J. C.; "Catalytic and structural properties of ruthenium bimetallic catalysts: effects of pretreatment on the behaviour of various Ru/Al<sub>2</sub>O<sub>3</sub> catalysts in alkane hydrogenolysis," *J. Mol. Catal.* 96, 163-173 (1995)
- Dorling, T. A., Eastlake, M. J., Moss, R. L.; "The Structure and Activity of Supported Metal Catalysts IV. Ethylene Hydrogenation on Platinum/Silica Catalysts," *J. Catal.*, 14, 23-33 (1969)
- Gates, B. C. in *Catalysis by Di- and Polynuclear Metal Cluster Complexes*, Adams, R. D., Cotton, F. A. Eds.; "Metal Cluster Catalysts Dispersed on Solid Supports," Wiley-VCH, Weinheim, pp. 509 (1998)
- George, G. N., George, J. S., Pickering, I. J.; "EXAFSPAK: A Suite of Computer Programs for Analysis of X-ray Absorption Spectra," Stanford Synchrotron Radiation Laboratory, Stanford Linear Accelerator Center, (2000); Home page, <http://www-ssrl.slac.stanford.edu/exafspak.html> (downloaded 2004)
- Hadjiivanov, K. I., Vayssilov, G. N. in *Advances in Catalysis Volume 47*, Gates, B. C., Knözinger, H. Eds.; "Characterization of Oxide Surfaces and Zeolites by Carbon Monoxide as an IR Probe Molecule" Academic Press, Amsterdam, pp. 451-480 (2002)
- Hwang, K. S., Yang, M., Xhu, J., Grunes, J., Somorjai, G. A.; "The Molecular Mechanism of the poisoning of platinum and rhodium catalyzed ethylene hydrogenation by carbon monoxide," *J. Mol. Catal.*, 204-205, 499-507 (2003)
- Jentoft, R. E., Deutsch, S. E., Gates, B. C.; "Low-cost, heated, and/or cooled flow-through cell for transmission x-ray absorption spectroscopy," *Rev. Sci. Instrum.*, 67, 2111-2112 (1996)
- Mestl, G. and Knözinger, H., in *Handbook of Heterogeneous Catalysis*, Ertl, G., Knözinger, H., and Weitkamp, J., Eds; "Vibrational Spectroscopies," VCH Verlagsgesellschaft mbH, Weinheim, Germany, pp.563-568 (1997)
- Myllyoja, S., Suvanto, M., Kurhinen, M., Hirva, P., Pakkanen, T. A., "Interactions of M(CO)<sub>6</sub> (M=Cr, Mo, W) with surface sites of Al<sub>2</sub>O<sub>3</sub>: a theoretical study," *Surf. Sci.*, 441, 454-460 (1999)
- Raval, B., Home page, <http://feff.phys.washington.edu/~raval/software/exafs/aboutathena.html> (downloaded 2003)
- Rehr, J. J., Mustre de leon, J., Zabinsky, S. I., Albers, R. C.; "Theoretical x-ray absorption fine structure standards," *J. Am. Chem. Soc.* 113, 5135 (1991)
- Shelef, M., Graham, G. W.; "Why rhodium in automotive three-way catalysts?," *Catal. Rev-Sci. Eng.* 36, 433-457 (1994)
- Vaarkamp, M., Linders, J. C., Koningsberger, D. C.; "A new method for parameterization of phase shift and backscattering amplitude," *Physica B*, 208-209 159-160, (1995)